Highly Efficient Removal of Perfluorooctanoic Acid from Water using Zirconium Terephthalate (UiO-66) Gel

Giuseppe Di Palma,*[a] Pritam Banerjee,[a] Kasper Enemark-Rasmussen,[b] Sara Talebi Deylamani[a] and Joerg R. Jinschek*[a]

[*] Dr. G. Di Palma, Dr. P. Banerjee, S. Talebi Deylamani, Professor J. R. Jinschek
National Centre for Nano Fabrication and Characterization
(DTU Nanolab)
Technical University of Denmark
Fysikvej 307, Kongens Lyngby DK-2800, Denmark
E-mail (corresponding authors): gdipa@dtu.dk; jojin@dtu.dk

[b] Dr. K. Enemark-Rasmussen,
Department of Chemistry, Technical University of Denmark, Kongens Lyngby, Denmark

Supporting information for this article is given via a link at the end of the document

Abstract: The extensive use and environmental release of perfluoroalkyl substances (PFAS), often referred to as “forever chemicals”, has raised significant health and environmental concerns. Due to their persistence and resistance to natural degradation, PFAS appear in concerningly high concentrations, e.g., in our drinking water. Among these substances, perfluorooctanoic acid (PFOA) is particularly prevalent. This study explores the application of synthesized zirconium terephthalate (UiO-66) metal-organic framework (MOF) gel for highly efficient removal of PFOA from water. The UiO-66 gel not only maintains the structural stability of its powder form but also offers improved ease of handling. Structural characterization by PXRD and TEM analyses revealed the gel's nanocrystalline structure (~20 nm in size), which was further confirmed by electron diffraction. Quantitative NMR spectroscopy demonstrated a PFOA removal efficiency of 96%. The successful absorption of the polyfluoro compound into the UiO-66 gel after filtration was confirmed by the detection of fluoride within the gel structure using STEM-EDS elemental mapping. In addition, to demonstrate the potential of developing membrane platforms as practical and scalable solutions for environmental remediation, the performance of a MOF gel filter was successfully tested.

The increasing prevalence of perfluoroalkyl substances (PFAS), a class of molecules used in our society since the 1940s for their chemical stability, has raised significant health and environmental concerns due to their persistence and widespread use[1]. These chemicals, often called 'forever chemicals,' persist in the environment due to their resistance to natural degradation.[2] PFAS contamination occurs mainly in surface waters and therefore also leads to contamination in foods such as fish and seafood.[2] Among these PFAS molecules, perfluorooctanoic acid (PFOA) is one of the most commonly used. Given the urgency, practical solutions are needed to remove PFOA from contaminated water, ensuring the access to safe drinking water and effective wastewater treatment.

Metal organic frameworks (MOFs), are known as extensive crystalline materials[3–6] with immense applicability in many fields[7–9] such as catalysis[10,11], gas separation[12], sensing[13–15] and molecular sieving[16]. Another significant application is their use in pollutant removal in water[17] and air[18] and specifically for the harvesting of PFAS[19–23]. Their primary applicability relies on producing a microcrystalline powder, limiting their use in platforms that require increased packeting therefore hindering a scalability as filter membranes.

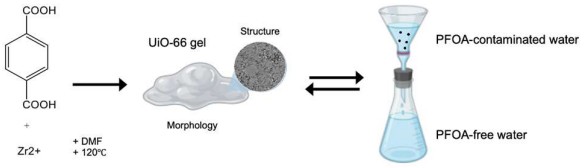

Figure 1. Schematic illustration of the study: Zr-terephthalate gel, UiO-66, was developed and used as a membrane material to effectively remove hazardous "forever chemical" PFOA from water.

Zhou et al.[22,24] have reported the molecular mechanism of MOFs to harvest PFAS, while Wong et al. have shown the importance of a high defect density in the MOF structure to enhance PFOA harvesting.[25] However, MOFs in powder form still have several disadvantages in practical applications.[26] They exhibit poor processability and handling[27] and poor hierarchical pore control due to their extensive crystalline structure.[28], mass transfer limitations in packed beds and columns[27,28], and limitations in assembly into practical devices due to the limited mechanical support of the microcrystalline powder[29]. Over the years, scientists have investigated MOF in gel form rather than in powder form as these gels can as well self-assemble into discrete crystalline nanoparticles[30], forming a colloidal network that aggregates in a liquid phase[31]. MOF-gels represent a highly defective and hierarchical porous structures[32–34] and thereby exhibit enhanced performance in catalysis and gas storage[35], better mechanical stability compared to MOF-powders[28] and high versatility in forming into various shapes such as coatings, films, membranes, and monoliths[27,28,36].

In the field of water filtration, methods such as ultrafiltration represent a versatile method that can effectively harvest several pollutants[37,38]. However, to be efficient, ultrafiltration must be performed at lower transmembrane pressure, increasing concerns about cost and maintenance required to maintain vacuum[39,40].

Lastly, in the field of PFAS degradation, two studies investigated photocatalysis for the defluorination of PFAS[41,42] at low temperature, advancing the field by providing a relative simple and inexpensive degradation of these compounds. However, the PFAS accumulation that triggers these reactions still remain an unsolved problem. A method for their initial accumulation is crucial to use in combination with effective PFAS degradation[43].

Here, we propose to combine the advantages of easy handling of MOF-gels to capture PFOA with high efficiency using a platform that allows fast and cost-effective pollutant removal and accumulation. In our study, we investigate the structural properties of the MOF-gel before and after filtration of PFOA-contaminated water, the distribution of adsorbed PFOA, and the efficiency of pollutant removal. The gel's porous structure and nano crystallinity were confirmed by Powder X-ray Diffraction (PXRD) as well as electron diffraction (ED). The gel was then immersed into a controlled PFOA solution, and Fluoride Nuclear Magnetic Resonance (19F-NMR) was used to analyze the supernatant to assess the pollutant harvesting performance. Solid-state NMR provided further insights into the interaction between the fluorinated compound and the gel matrix, shedding lights into the nature of these bindings. Elemental mapping by Energy Dispersive Spectroscopy (EDS) in scanning electron microscopy (STEM) was applied to confirm the ability of the gel to absorb PFOA, to visualize the spatial distribution of PFOA within the gel, and to verify the uptake on the nanoscale. Finally, to prove that the gel could function as a PFOA accumulator, the gel was used as a filter and the contaminated water was passed through to test the scalability of the approach proposed here. Our results prove that MOF-gels, such as UiO-66 gel, can provide an efficient and scalable platform for PFAS remediation, and pave the way for new practical solutions for these environmental challenges.

As the initial step, zirconium terephthalate gel (UiO-66 gel) was synthesized by mixing zirconium oxide chloride octahydrate and terephthalic acid in dimethylformamide (DMF) with acetic acid as modulator and left overnight in an oven at 120° C (see *SI* for further details). The subsequent washing procedure, with DMF first and water second to remove the non-react residues, formed a gel separated from the solvent. PXRD and TEM studies were performed to investigate the morphology of the gel in a dry state. PXRD (see Figure S1 in *SI*) showed a broad peak at around 5 degrees. This peak broadening indicates that the colloidal particles are very small (in the nanometer range) and therefore below the detection limits of PXRD but still indicating a discrete ordering in the material. ED in TEM (Figure 2a) shows distinct rings confirming the crystalline nature of the UiO-66 gel. The high-angle annular dark field (HAADF) STEM image in Figure 2b reveals a hierarchical porous structure of the gel. The corresponding STEM-EDS elemental mapping of zirconium (Figure 2d) and oxygen (Figure 2e) showed a complementary distribution, as expected for zirconium oxocluster in UiO-66. After

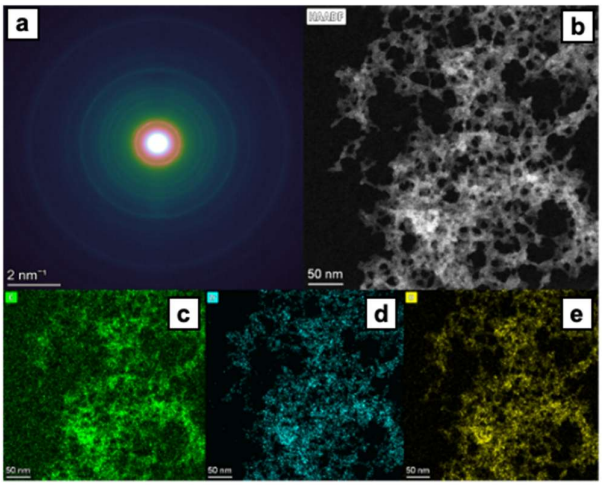

Figure 2. TEM analysis of the as-synthesized UiO-66 gel. (a) Electron diffraction (SAED) of the gel showing diffraction rings typical of nanocrystalline materials; (b) HAADF-STEM image showing the hierarchical structure of the material; (c)-(d): Corresponding elemental mapping by STEM-EDS, (c) Carbon (green), (d) Zirconium (light blue), (e) Oxygen (yellow)

this, the PFOA harvesting capacity of the gel was investigated. 1.6 grams of gel (wet state) were immersed into a 10 ml solution of 2.37 mM PFOA, mixed, and left overnight. After the gel was separated by centrifugation, the supernatant was analyzed with ^{19}F NMR spectroscopy. ^{19}F NMR (Figure 3) was employed to detect PFOA, because fluoride traces are only present in PFOA due to the lack of C-H groups. The peak ⑦ at -80.75 ppm was

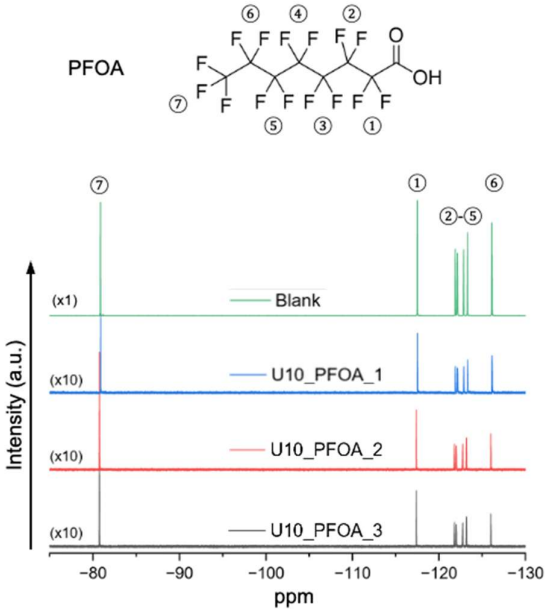

Figure 3. 19F NMR of the PFOA (#①-⑦ indicate the different C-F terminal groups) in the supernatant before (green) and after contact with UiO-66 (blue, red and black) collected as triplicate. Peaks in the NMR spectra corresponding to the different C-F terminal groups are indicated by corresponding #s ①-⑦) The change in intensity of peak ⑦ at -80.75 ppm was used to calculate the harvesting efficiency (see details in *SI*: table in Figure S2).

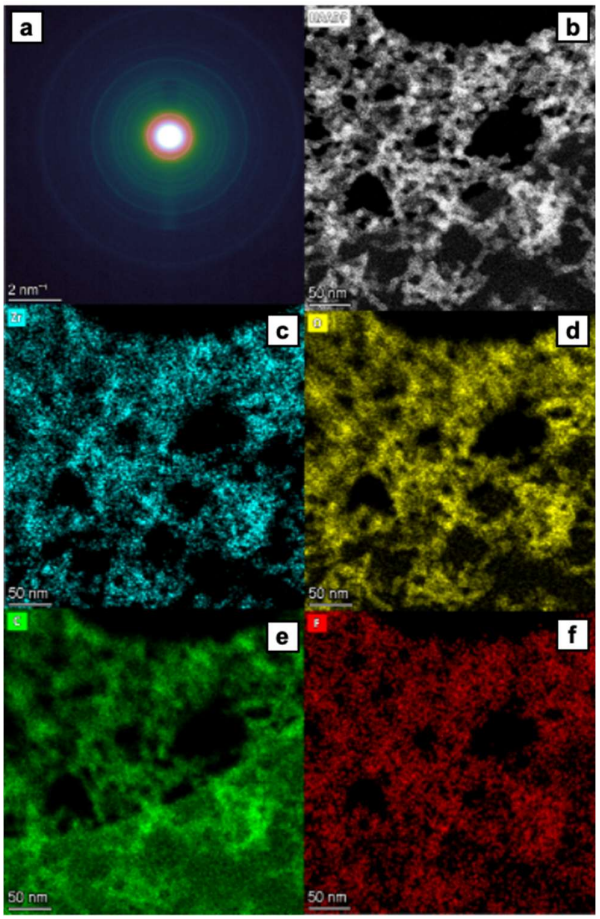

Figure 4. TEM analysis of the UiO-66 gel after contact with PFOA. The electron diffraction (ED) pattern in (a) and the HAADF-STEM image in (b) confirm the crystalline and hierarchical pores structure of the MOF gel. (c)-(f): Elemental mapping analysis of the UiO-66 components using STEM-EDS; showing the mapping of (c) Zirconium (light blue), (d) Oxygen (yellow), (e) Carbon (green), and (f) Fluoride (red). The complementarity of the fluoride signal in (f) with the other elements (c-e) indicates the absorption of the PFOA in the matrix of the MOF gel.

assigned to the CF3 terminal group of the PFOA, while the peak ⑥ at -126.7 ppm was assigned to the CF_2 moiety next to the acid, according to previous literature[44]. The calculated area of the peak showed a generally reduced peak intensity compared to the blank (see details in the table in Figure S2 in *SI*, column: CF3 peak area), strongly indicating that PFOA was removed from the water when the gel was present. The gel achieved a harvesting efficiency (HE) of 96.2(±0.2) %, reducing PFOA concentration from 2.360 mM to 0.089(±0.005) mM in a single cycle (see details in the table in Figure S2 in *SI*), demonstrating its promising potential for water ultrafiltration. Solid-state ^{19}F MAS and ^{13}C-{^{19}F} CPMAS NMR spectra confirm the presence of PFOA inside the dried spent gel (see Figure S3 in *SI*). While the 13C spectrum of the dried gel is almost identical to the reference PFOA (see right figure in Figure S3 in *SI*), the 19F spectrum is less resolved, for the CF2 moieties (see peaks at -125ppm in left figure in Figure S3 in *SI*). Although the CF_3 peak exhibits a slight shift towards less negative ppm, the broadening of the CF_2 signals and absence of

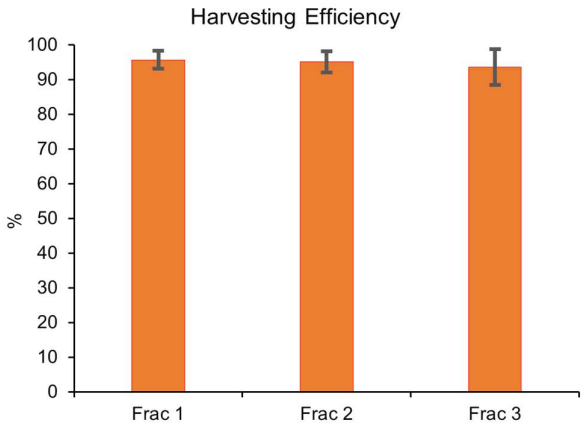

Figure 5. Harvesting efficiency of the UiO-66 gel after the first (Frac1), second (Frac 2) and third fraction (Frac 3).

the CF_2 at -126 ppm (see left figure in Figure S3 in *SI*) suggests that the PFOA coordinates to the carbonyl end of UiO-66 (i.e. the zirconium oxo cluster). Ultimately, the observation of the ^{13}C chemical shift of the carbonyl supports this interpretation. However, the PFOA concentration in the used gel was too low to detect a ^{13}C spectrum with sufficient S/N ratio to identify the carbonyl signal, which is only weakly observed for the reference PFOA at 168 ppm in the ^{13}C-{^{19}F} CPMAS experiment (see Figure S3 in *SI*). TEM analysis (Figure 5) was performed on the dry gel after contact with PFOA. TEM-ED analysis (Figure 4a) confirmed that UiO-66 gel retained its crystalline structure and hierarchical pores after PFOA contact, as shown by unchanged ED patterns (see Figure S4 in *SI*). Scanning Electron microscope (SEM) pictures showed no apparent change in gel morphology before and after the PFOA contact (see Figure S5 in *SI*). The STEM-EDS mapping (Figures 4b-f) showed a spatially homogeneous fluoride signal throughout the UiO-66 matrix, confirming that the fluorine compound has interacted with the gel as the molecules are absorbed in the gel framework. STEM-EDS spot analysis of the gel after PFOA contact shows a significant F peak, in contrast to the gel before the contact with PFOA (no F peak, see details in Figure S6 in *SI*).

Finally, we form the UiO-66 gel into a membrane to test the scalability of the here proposed concept for water filtration. To create the membrane, the gel was dispersed in ethanol and applied to a filter paper. The filtration efficiency was tested with 3 fractions of 6 ml PFOA-water solution (2.36mM) to evaluate the suitability of the gel as a membrane for the ultrafiltration of PFOA-contaminated water. Again, ^{19}F NMR and the peak at 80.75 (see ⑦ in Figure 3) was used to estimate the concentration of PFOA in water, before and after contact with the gel, respectively. The first, second and third fraction's calculated concentration after gel contact was 0.10 mM (Frac 1), 0.11 mM (Frac 2), and 0.15 mM (Frac 3), marking a HE at 95.0 % ±1.3%, 95.0% ±1.5% and 93.5% ±2.5%, respectively (Figure 5). It is worth noting that it took only a few minutes for each fraction to pass through the gel membrane and the funnel, and the pollutant separation occurred solely due to gravity. This indicates a higher performance in the initial filtration of water, as traditional filtration methods[45] require a

differential in pressure for the water to pass through a membrane. Therefore, our proposed method would allow for lower cost and less maintenance compared to traditional methods, and the increased HE in the three fractions (Figure 5) showed a potential for few replacements of the filter system. Thus, our UiO-66 gel membrane represents a scalable solution for the remediation of PFAO-contaminated water, offering both efficiency and applicability in large-scale water treatment.

In conclusion, our study demonstrates the potential of zirconium terephthalate gels as a valuable material for water ultrafiltration, especially for PFAS removal. The gel morphology addresses limitations of MOFs in powder form, offering easy handling as well as better mechanical support and processability. By a detailed characterization using PXRD and a suite of TEM-based techniques, such as electron diffraction and STEM imaging, the gel possessed a nanocrystalline character and hierarchical porous structure, which is crucial for its functionality in pollutant removal. Quantitative NMR revealed that the gel achieved an efficiency of ~96%, while solid-state NMR proved the interaction of the fluoride groups with the gel matrix. Furthermore, HAADF-STEM imaging as well STEM-EDS elemental mapping revealed that, while the gel maintained its microstructure, the PFOA is evenly distributed within the gel after application. After the UiO-66 gel was used (as membrane) for water ultrafiltration it maintained high harvesting ability with an HE above 95%. This highlights the potential of MOF gels as scalable platforms for environmental remediation.

Thanks to their improved handling, high pollutant removal efficiency and structural stability, MOF gels show great promise in terms of sustainability in addressing environmental challenges.

Acknowledgements

The authors acknowledge funding from the Novo Nordisk Foundation (Project “Electron Microscopy of Dynamical Processes” NNF21OC0072844). The NMR Center at DTU and the Villum Foundation are acknowledged for access to the 600 and 800 MHz spectrometers.

Keywords: PFAS • MOF • water remediation • PFOA removal

[1] J. R. Baran, *J. Am. Chem. Soc.* **2001**, *123*, 8882–8882.
[2] H. Brunn, G. Arnold, W. Körner, G. Rippen, K. G. Steinhäuser, I. Valentin, *Environmental Sciences Europe* **2023**, *35*, 20.
[3] O. K. Farha, J. T. Hupp, *Acc. Chem. Res.* **2010**, *43*, 1166–1175.
[4] V. F. Yusuf, N. I. Malek, S. K. Kailasa, *ACS Omega* **2022**, *7*, 44507–44531.
[5] D. Li, A. Yadav, H. Zhou, K. Roy, P. Thanasekaran, C. Lee, *Global Challenges* **2024**, *8*, 2300244.
[6] H.-C. Zhou, J. R. Long, O. M. Yaghi, *Chem. Rev.* **2012**, *112*, 673–674.
[7] H. Li, M. Eddaoudi, M. O’Keeffe, O. M. Yaghi, *Nature* **1999**, *402*, 276–279.
[8] R.-B. Lin, Z. Zhang, B. Chen, *Acc. Chem. Res.* **2021**, *54*, 3362–3376.
[9] H. Furukawa, K. E. Cordova, M. O’Keeffe, O. M. Yaghi, *Science* **2013**, *341*, 1230444.
[10] J. Lee, O. K. Farha, J. Roberts, K. A. Scheidt, S. T. Nguyen, J. T. Hupp, *Chem. Soc. Rev.* **2009**, *38*, 1450–1459.
[11] B. Zhu, R. Zou, Q. Xu, *Advanced Energy Materials* **2018**, *8*, 1801193.
[12] J.-R. Li, R. J. Kuppler, H.-C. Zhou, *Chem. Soc. Rev.* **2009**, *38*, 1477–1504.
[13] L. E. Kreno, K. Leong, O. K. Farha, M. Allendorf, R. P. Van Duyne, J. T. Hupp, *Chem. Rev.* **2012**, *112*, 1105–1125.
[14] W. P. Lustig, S. Mukherjee, N. D. Rudd, A. V. Desai, J. Li, S. K. Ghosh, *Chem. Soc. Rev.* **2017**, *46*, 3242–3285.
[15] A. Zuliani, N. Khiar, C. Carrillo-Carrión, *Anal Bioanal Chem* **2023**, 1–19.
[16] Y. Peng, Y. Li, Y. Ban, H. Jin, W. Jiao, X. Liu, W. Yang, *Science* **2014**, *346*, 1356–1359.
[17] H. Kaur, N. Devi, S. S. Siwal, W. F. Alsanie, M. K. Thakur, V. K. Thakur, *ACS Omega* **2023**, *8*, 9004–9030.
[18] Y. Jin, H. Liu, M. Feng, Q. Ma, B. Wang, *Advanced Functional Materials* **2024**, *34*, 2304773.
[19] L. I. FitzGerald, J. F. Olorunyomi, R. Singh, C. M. Doherty, *ChemSusChem* **2022**, *15*, e202201136.
[20] K. Sini, D. Bourgeois, M. Idouhar, M. Carboni, D. Meyer, *New J. Chem.* **2018**, *42*, 17889–17894.
[21] E. Loukopoulos, S. Marugán-Benito, D. Raptis, E. Tylianakis, G. E. Froudakis, A. Mavrandonakis, A. E. Platero-Prats, *Advanced Functional Materials* **2024**, *34*, 2409932.
[22] R.-R. Liang, S. Xu, Z. Han, Y. Yang, K.-Y. Wang, Z. Huang, J. Rushlow, P. Cai, P. Samorì, H.-C. Zhou, *J. Am. Chem. Soc.* **2024**, *146*, 9811–9818.
[23] R. Li, S. Alomari, R. Stanton, M. C. Wasson, T. Islamoglu, O. K. Farha, T. M. Holsen, S. M. Thagard, D. J. Trivedi, M. Wriedt, *Chem. Mater.* **2021**, *33*, 3276–3285.
[24] R.-R. Liang, Y. Yang, Z. Han, V. I. Bakhmutov, J. Rushlow, Y. Fu, K.-Y. Wang, H.-C. Zhou, *Advanced Materials* **2024**, *36*, 2407194.
[25] C. A. Clark, K. N. Heck, C. D. Powell, M. S. Wong, *ACS Sustainable Chem. Eng.* **2019**, *7*, 6619–6628.
[26] Q. Ma, T. Zhang, B. Wang, *Matter* **2022**, *5*, 1070–1091.
[27] B. Bueken, N. V. Velthoven, T. Willhammar, T. Stassin, I. Stassen, D. A. Keen, G. V. Baron, J. F. M. Denayer, R. Ameloot, S. Bals, D. D. Vos, T. D. Bennett, *Chemical Science* **2017**, *8*, 3939–3948.
[28] J. Hou, A. F. Sapnik, T. D. Bennett, *Chemical Science* **2020**, *11*, 310–323.
[29] W. Cao, Z. Lin, D. Zheng, J. Zhang, W. Heng, Y. Wei, Y. Gao, S. Qian, *J. Mater. Chem. B* **2023**, *11*, 10566–10594.
[30] A. F. Sapnik, C. Sun, J. E. M. Laulainen, D. N. Johnstone, R. Brydson, T. Johnson, P. A. Midgley, T. D. Bennett, S. M. Collins, *Commun Chem* **2023**, *6*, 1–12.
[31] J. Troyano, A. Carné-Sánchez, C. Avci, I. Imaz, D. Maspoch, *Chem. Soc. Rev.* **2019**, *48*, 5534–5546.
[32] H. Qin, J. Sun, X. Yang, H. Li, X. Li, R. Wang, S. He, C. Zhou, *Journal of Colloid and Interface Science* **2024**, *655*, 23–31.
[33] D. Gao, J. Tang, F. Zhang, C. Wen, L. Feng, C. Wan, F. Qu, X. Liang, *Journal of Colloid and Interface Science* **2023**, *650*, 19–27.
[34] W. Zhang, Y. Liu, H. S. Jeppesen, N. Pinna, *Nat Commun* **2024**, *15*, 5463.
[35] R. He, J. He, J. Shen, H. Fu, Y. Zhang, B. Wang, *ss* **2024**, *4*, N/A-N/A.
[36] P. Albacete, M. Asgari, Y. Yang, A. N. Al-Shanks, D. Fairen-Jimenez, *Advanced Functional Materials* **2024**, *34*, 2305979.
[37] J. Xie, Z. Liao, M. Zhang, L. Ni, J. Qi, C. Wang, X. Sun, L. Wang, S. Wang, J. Li, *Environ. Sci. Technol.* **2021**, *55*, 2652–2661.
[38] S. Pan, J. Li, O. Noonan, X. Fang, G. Wan, C. Yu, L. Wang, *Environ. Sci. Technol.* **2017**, *51*, 5098–5107.
[39] M. Li, K. Zuo, S. Liang, K. Xiao, P. Liang, X. Wang, X. Huang, *Environ. Sci. Technol.* **2020**, *54*, 11536–11545.
[40] F. Meng, S. Zhang, Y. Oh, Z. Zhou, H.-S. Shin, S.-R. Chae, *Water Research* **2017**, *114*, 151–180.
[41] H. Zhang, J.-X. Chen, J.-P. Qu, Y.-B. Kang, *Nature* **2024**, *635*, 610–617.
[42] X. Liu, A. Sau, A. R. Green, M. V. Popescu, N. F. Pompetti, Y. Li, Y. Zhao, R. S. Paton, N. H. Damrauer, G. M. Miyake, *Nature* **2024**, 1–3.
[43] R.-R. Liang, Y. Fu, Z. Han, Y. Yang, V. I. Bakhmutov, Z. Liu, J. Rushlow, H.-C. Zhou, *Nat Water* **2024**, *2*, 1218–1225.
[44] R. E. Lewis, C.-H. Huang, J. C. White, C. L. Haynes, *ACS Nanosci. Au* **2023**, *3*, 408–417.
[45] B. Li, K. M. Dobosz, H. Zhang, J. D. Schiffman, K. Saranteas, M. A. Henson, *Chem Eng Sci* **2019**, *208*, 115162.

Entry for the Table of Contents

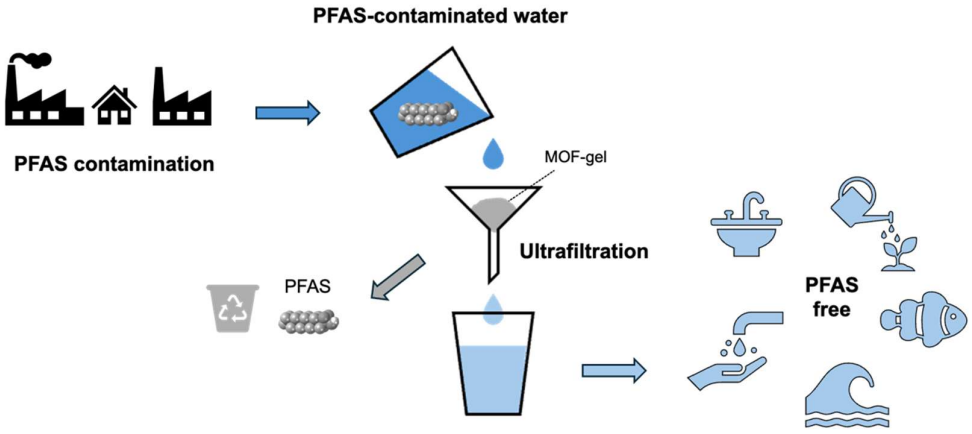

Graphical concept of this study. A MOF-gel membrane has been developed to filter PFAS (e.g., PFOA) from contaminated water, enabling PFAS capture and recycling, while recovering purified water for reuse in the hydric system.